Dual Cross-linking of Epoxidized Linseed Oil with Combined Aliphatic/Aromatic Diacids Containing Dynamic S–S Bonds Generating Recyclable Thermosets

Thi-Nguyet Tran, Chiara Di Mauro, Samuel Malburet, Alain Graillot, Alice Mija

HAL Id: hal-03006114
https://hal.univ-cotedazur.fr/hal-03006114

Submitted on 27 Jan 2021

Dual Cross-linking of Epoxidized Linseed Oil with Combined Aliphatic/Aromatic Diacids Containing Dynamic S−S Bonds Generating Recyclable Thermosets

Thi-Nguyet Tran, Chiara Di Mauro, Samuel Malburet, Alain Graillot, and Alice Mija*

Cite This: https://dx.doi.org/10.1021/acsabm.0c00788

Read Online

ACCESS | Metrics & More | Article Recommendations | Supporting Information

ABSTRACT: The end-of-life of thermoset materials is a real issue that confronts our society, and the strategy of introducing dynamic reversible bonds can be a sustainable solution to overcome this problem. This study shows an efficient way to produce biobased and recyclable thermosets, for a circular use. To reduce the production costs linked to energy and duration, an improved curing process is proposed by combining aromatic and aliphatic diacid hardeners containing dynamic S−S bonds. The work demonstrates the increased reactivity of epoxidized vegetable oil reacted with the two diacids. The structural evolutions during the exchange reactions that allow the recyclability were followed by Fourier transformed-infrared and nuclear magnetic resonance spectroscopies, high-performance liquid chromatography, and mass spectroscopy. The curing process was studied by differential scanning calorimetry and kinetic study.
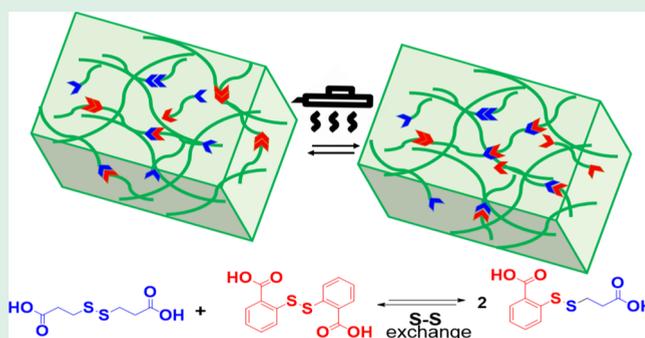
INTRODUCTION

The renewable resources represent important alternatives to fossil feedstocks to ensure a sustainable economy in times of growing world population and rising ecological awareness. The use of vegetable oils (VOs) as raw materials continues to be of great interest because of their universal availability, advantageous costs, and biodegradability.[1−6] Among several derivatives prepared from VOs, the presence of reactive functional groups, together with the possibility to produce it at a large scale, make the epoxidized vegetable oils (EVOs) extremely attractive as green monomers for the biobased thermosetting resin market.[7−10] Their only drawback is low reactivity, due also to the internal position of epoxide groups.[11,12] The EVO homopolymers generally exhibit low performance in terms of glass transition (T_g), strengths, and moduli because of their long fatty chain-constituting structure. However, the EVOs curing with appropriate cross-linkers can generate thermosets with good thermomechanical properties. Among several classes of cross-linkers, the dicarboxylic acids (DCA), in particular the aliphatic DCA, are the second most popular hardeners for epoxy resins after the amines because of their low toxicity, relatively low price, and availability. These aliphatic hardeners produce thermosets with good flexibility and weatherability properties. Ding *et al.*[8] reported the curing of the epoxidized linseed oil (ELO) monomer with aliphatic diacids having different chain lengths, from C_6 to C_{18}. The authors showed

that a shorter diacid chain, as C_6, has an increased reactivity toward the epoxide groups and therefore a low reaction activation energy. At the same time, the resins obtained with a short DCA chain length exhibited high T_g and good mechanical properties, including tensile strength, tensile strain, modulus, and toughness but exhibited poor thermal stability. Similar trends were reported by Run-Tao *et al.*[13] on the curing of epoxidized soybean oil (ESO) with several aliphatic DCA including adipic acid (AA, C_6), sebacic acid (SA, C_{10}), and 1,12-dodecanedicarboxylic acid (DA, C_{12}). However, the common challenge of these conventional thermosets is material durability and the difficulty of reprocessing. Nowadays, the problems linked to the materials' end-of-life related to waste disposal, and so forth, force academic and industrial researchers to find sustainable solutions concerning the durability and the reprocessing of materials.[14−20] During the last decade, many researches focused on materials being able to fully, or partially, restore their physical and mechanical

properties after suffering different types of damages by using different approaches.[21,22]

One of the most interesting strategies is to introduce dynamic and/or reversible chemical bonds in the polymeric structure, at which the networks can rearrange their topologies *via* exchange reactions under external stimuli such as heat or UV irradiation.[23−25] This dynamic process allows the material to exhibit properties such as self-healing, recyclability/reprocessability, and/or improved processability.[26] Among various dynamic covalent bonds, the disulfide linkage is one of the most used because of a wide range of commercially available products. Therefore, the polymer architectures having incorporated S−S bonds have their responsiveness toward various external stimuli activated at moderate temperatures without any catalyst or initiator.[27−30] Furthermore, S−S bonds are weaker than C−C ones, therefore, the dynamic linkages can be used to strategically introduce dynamic connections into a thermosetting resin. In this regard, the objective of this study is to build high-performance and reprocessable EVO-based thermoset networks by using DCA-containing S−S bonding in their structures as cross-linkers. As a biobased epoxy monomer, the ELO was chosen because of its availability in the market and high epoxy content.

A challenging aspect in the thermosetting resins is the difficulty in combining mechanical properties and reprocessing performances. To overcome this limitation, combining different cross-linkers seems to be a promising strategy allowing to modulate not only good mechanical performances but also the reprocessing ability. This method is frequently used in the resin industry market. Matxain *et al.*[25] carried out theoretical calculations on a wide set of different disulfide compounds, both aliphatic and aromatic. The authors noticed that the bond dissociation energy (BDE) of disulfide bonds can be greatly reduced due to the presence of aromatic rings. It means that the reversible recombination of disulfide bonds can occur more easily and more efficiently in the case of aromatic disulfide compounds.

In light of these considerations, the aim of this study is to design a dual reversible cross-linked network based on ELO reacted with an aromatic BA, 2,2′-dithiodibenzoic acid, and/or with an aliphatic DA with a short chain, 3,3′-dithiodipropionic acid (DA, C_6). The use of both disulfide-containing hardeners: aromatic and aliphatic can achieve the desirable combinations in material properties and processability. Moreover, the strategy of double aliphatic/aromatic cross-linking, with different reactivities of the monomer toward the two hardeners, can open the door to novel materials with unique mechanical properties, as applied, for example, to produce super-tough hydrogels with strong interfacial adhesion.[31,32]

The addition of BA as an aromatic diacid in the ELO matrix will not only introduce its rigid structure into the network, increasing the mechanical properties, but also will incorporate aromatic disulfide bonds with low BDE, allowing to accelerate the disulfide metathesis reactions, therefore enhancing the reprocessing ability of final materials. The mechanism responsible for the self-healing process in disulfide-based materials has been discussed in recent literature,[25,33−37] both theoretically and experimentally. A [2 + 1] radical-mediated mechanism is found to be responsible for the self-healing reaction and not the expected [2 + 2] metathesis mechanism. According to the authors, in the [2 + 1] mechanism, the first step is the generation of sulfenyl radicals by the cleavage of the S−S bond that attacks other disulfide bonds that are found in

the vicinity, leading to the interchange of the sulfur atoms in the process, as shown in Scheme 1.

Scheme 1. Schematic Representation of [2 + 2] Metathesis (above) and [2 + 1] Radical-Mediated (below, Dominant Mechanism) Reaction Mechanisms[25,33,34]
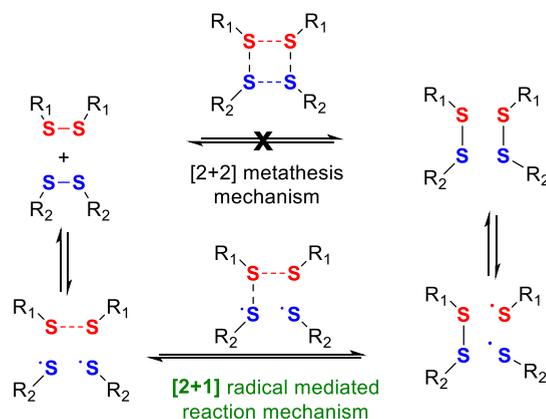
■ RESULTS AND DISCUSSION

Studies on Cross-linking Reactivity. The reactivity of the ELO monomer in combination with DCA, including DA and BA, to form epoxy thermosets was studied by differential scanning calorimetry (DSC), Fourier transform infrared (FT-IR), and nuclear magnetic resonance (NMR). The proposed mechanism of reactions is schematized and presented in Scheme 2. To ensure a complete reaction of all epoxy functionalities, a ratio of 1:1 epoxy/acid was selected, according to the sample preparation reported in Supporting Information. This ratio allows to achieve high selectivity of the copolymerization reaction and also better thermoset performances. As the initiator, the imidazole was chosen because of its high reactivity and relatively low cost,[8,38−41] and especially for its selectivity on the epoxy−acid copolymerization main reaction.[42] An imidazole ratio of 1 wt % of the total epoxy/hardener mixture was used. Five formulations are studied, as listed in Table 1. The acronyms of the formulations were abbreviated, in function of their compositions. For example, "ELO/DA$_{70}$BA$_{30}$" corresponds to the system with ELO mixed with 70 mol % of DA and 30 mol % of BA in the hardener composition mixture.

DSC Investigations. *Curing Behaviors.* To control in an appropriate way, the cross-linking process is a key issue to obtain good thermosetting resin properties. To evaluate the reactivity and the thermodynamic parameters of the cross-linking reaction, dynamic DSC analysis was used to follow the copolymerization of ELO with the two selected acids, individually and also with their mixtures. Two formulations were used as the control reference: ELO/DA$_{100}$ (100% aliphatic diacid − control 1) and ELO/BA$_{100}$ (100% aromatic diacid − control 2). The corresponding DSC thermograms of formulations heated at 10 °C min^{-1} are displayed in Figures 1 and in S1.

An endotherm peak at about 80−100 °C is attributed to the melting of imidazole before the exothermal, first order transition, which is attributed to the epoxy/diacid curing reaction. For the formulations having a percentage of the aromatic diacid (BA) superior to 50%, the initiator melting peak is diminished and difficult to be detected in DSC

Scheme 2. (a) Proposed Mechanism for the ELO/DCA Copolymerization in the Presence of Imidazole as an Initiator *via* Carboxylate Complex and (b) Schematic Representation of Obtained Network Containing Aromatic and Aliphatic Disulfide Segments
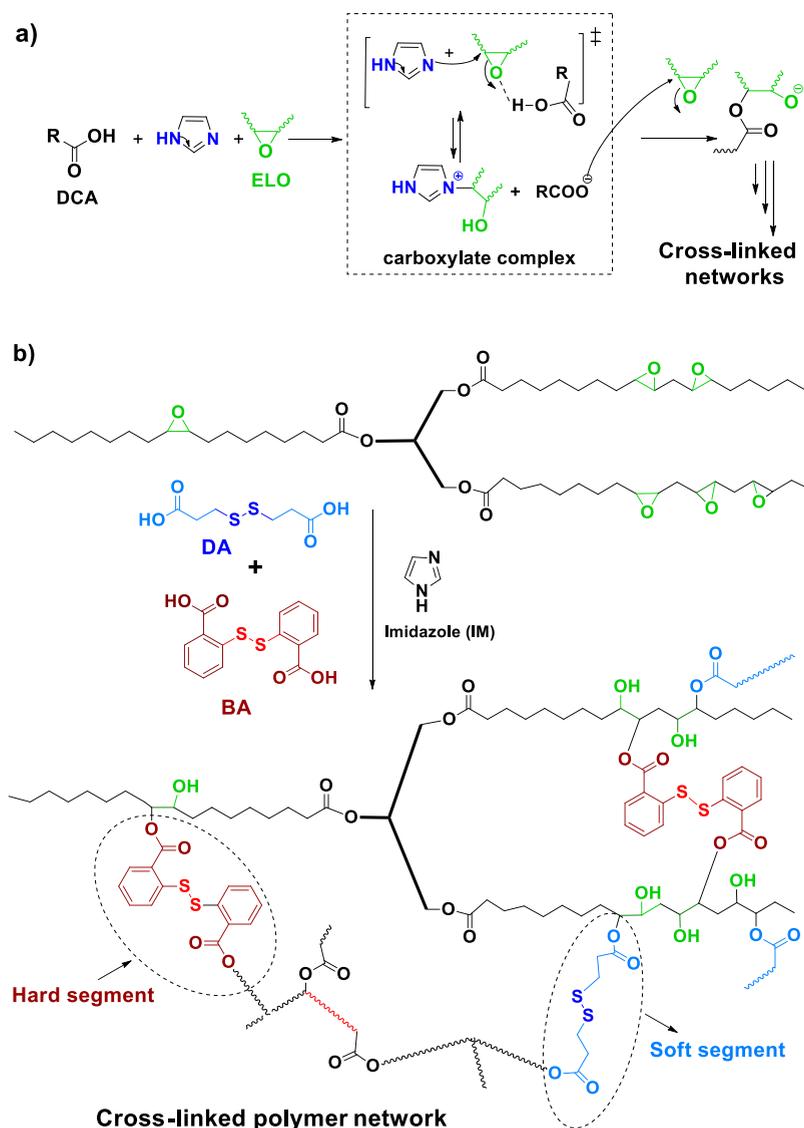
Table 1. Formulation Compositions Expressed in Molar Equivalent

formulations	ELO	DA[a]	BA[a]
ELO/DA$_{100}$ (control 1)	1	1	0
ELO/DA$_{70}$BA$_{30}$	1	0.7	0.3
ELO/DA$_{50}$BA$_{50}$	1	0.5	0.5
ELO/DA$_{30}$BA$_{70}$	1	0.3	0.7
ELO/BA$_{100}$ (control 2)	1	0	1

[a]Functional ratio in mol in total of carboxylic groups.

Figure 1. Dynamic DSC scans for ELO/DCA formulations, with imidazole as the initiator, during heating at 10 °C min^{-1}.

thermograms, as presented in Figures 1 and S1. This result can be associated with a higher interaction and compatibility of the imidazole with BA, and in consequence, its better dissolution in the initial stages of premixing.

As can be seen in Figure 1 and Table 2, the cross-linking process starts at about 118−133 °C and ends between 166 and 184 °C, depending on the formulation composition.

Comparing the DSC thermograms of the two control reference systems, ELO/DA$_{100}$ and ELO/BA$_{100}$, we can observe that the reaction onsets (T_{on}) are closed for both systems, while ELO/DA$_{100}$ exhibits a lower T_{peak} (142 *vs* 154 °C for aromatic acid), with a shorter interval of reaction (Table

Table 2. DSC Data of Reactivity Study of ELO/DCA Curing Formulations

curing mixture	T_{on} (°C)	T_{peak} (°C)	T_{end} (°C)	ΔT (°C)	ΔH (J g^{-1})	T_g (°C)[a]
ELO/DA$_{100}$ (control 1)	133	142	175	42	155 ± 2	7
ELO/DA$_{70}$BA$_{30}$	124	137	166	42	141 ± 2	20
ELO/DA$_{50}$BA$_{50}$	118	142	171	53	164 ± 2	33
ELO/DA$_{30}$BA$_{70}$	123	148	179	56	196 ± 2	49
ELO/BA$_{100}$ (control 2)	130	154	184	54	198 ± 2	76

[a]T_g values were measured by DSC on the cured thermosets.

2, ΔT = 42 *vs* 54 °C). However, regarding the shape of the DSC thermogram of the ELO/DA$_{100}$ system, it should be noted that its exothermal peak is not as symmetrical as that of the ELO/BA$_{100}$ system. Surprisingly, by adding BA in the DA/ELO mixture, the shape of the exotherm peak becomes symmetrical. It appears that this DSC profile is more complex, essentially because of decreasing reactivity after T_{peak}. Thereafter, we can notice that the DSC thermocuring curves show the presence of secondary reactions starting at high temperature, ≥195 °C, with a peak around 240 °C. The appearance of this second exothermic peak at higher temperatures could be attributed to the epoxide homopolymerization and/or etherification, occurring in competition to the main copolymerization reaction, according to Fringant and Boquillon[43] and to our previous studies.[42,44]

At the same time, it is worthy to note that the reaction peak temperature, representing the maximum reaction rate, shows a tendency to decrease with the DA % in the matrix. In fact, it changes from 154 °C for ELO/BA$_{100}$ (control 2) to around 137 °C when 70% mol of DA are added. These T_{peak} values decrease progressively with the percentage of DA: 148 °C for ELO/DA$_{30}$BA$_{70}$ and 142 °C for ELO/DA$_{50}$BA$_{50}$. This result suggests the good compatibility of BA and DA hardeners with ELO and that DA plays the role of a reactive compatibilizer.

Considering the values of reaction enthalpies, it shows the same tendency of T_{peak} values. As expected, a higher reaction enthalpy was obtained for the ELO/BA$_{100}$ (control 2) system with a value of 198 J g^{-1}, compared to 155 J g^{-1} for ELO/DA$_{100}$ (control 1). This observation is probably attributed to higher reactivity of aromatic diacid (BA) versus oxirane groups of the ELO monomer. Surprisingly, the lowest value of enthalpy (ΔH = 141 J g^{-1}) was found for ELO/DA$_{30}$BA$_{70}$ and not for the system with 100% DA, as we would have expected (ELO/DA$_{100}$, ΔH = 155 J g^{-1}). This result can be correlated to

the occurrence of a complex mechanism reaction, or perhaps not all the diacids were reacted during the thermocuring program. This complex mechanism is investigated in the next sections.

Regarding the onset reaction temperature (T_{on}) values of 5 formulations, from Figure 1, it is shown clearly that by mixing DA with BA, the T_{on} decreased significantly, compared to the two control systems. The lowest T_{on} value was detected for ELO/DA$_{50}$BA$_{50}$ formulation, around 118 °C.

Estimation of the Apparent Activation Energy, E_a. To study the diacid effect on ELO/DCA reactivity, dynamic DSC analyses for some selected formulations were performed at different heating rates. The activation energy (E_a) of the curing reaction was evaluated using Kissinger[45] (eq 1) and Ozawa[46] (eq 2) methods.

$$\ln\left(\frac{\beta}{T_{peak}^2}\right) = \ln\left(\frac{AR}{E_a}\right) + \frac{E_a}{RT_{peak}} \tag{1}$$

$$\ln\beta = -1.052\left(\frac{E_a}{RT_{peak}}\right) + \ln\left(\frac{AE_a}{R}\right) - \ln(F(x)) - 5.331 \tag{2}$$

where R is the universal gas constant, β is the heating rate, T_{peak} is the temperature of the exothermic peak, and $F(x)$ is a conversion-dependent term. By plotting $\ln(\beta/T_{peak}^2)$ versus $1/T_{peak}$ (Kissinger) and $\ln(\beta)$ versus $1/T_{peak}$ (Ozawa), the activation energy and the pre-exponential factor can be obtained by calculating the slope of the linear fit and the intercept, respectively.

Figure 2A shows the dynamic DSC scans of ELO/DA$_{50}$BA$_{50}$ formulation during heating at different heating rates. The analysis of the three formulation data (control 1, control 2, and ELO/DA$_{50}$BA$_{50}$) is given in Tables S2−S4. It is obvious that T_{peak} increases with the heating rate because of the thermal lag, as reported by Haines.[47] Using these DSC data, especially the reaction T_{peak}, the curing activation energies were determined by Kissinger and Ozawa methods. A typical plot presentation of the Kissinger method is displayed in Figure 2B. The corresponding values obtained after applying both methods are given in Table 3. According to Viska *et al.*,[48] the E_a calculated by the Kissinger method provided generally lower results than those obtained using the Ozawa method. The same results were obtained in our case for all systems. Both methods show a linear fitting for the studied formulations ($R^2 \geq 0.9175$) with E_a values in the range of 74−116 kJ mol^{-1}. These values are in the same range with those reported in the literature. Chen *et*
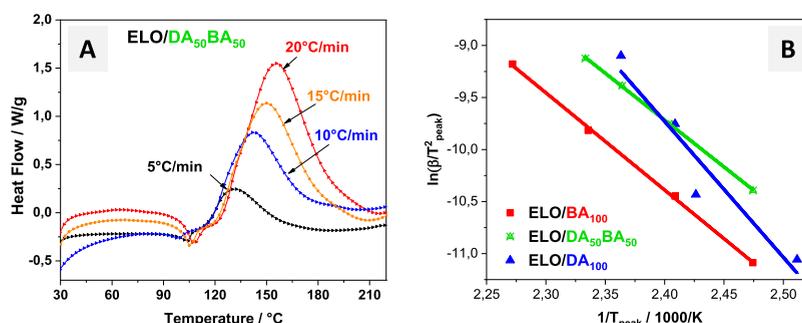
Figure 2. (A) Dynamic DSC thermograms of ELO/DA$_{50}$BA$_{50}$ at the indicated heating rates and (B) calculated reaction activation energy expressed in function of the reaction temperature peak, evaluated by DSC analysis.

Table 3. Calculated Reaction Activation Energy Using DSC Data[a]

	Kissinger method		Ozawa method	
formulations	E_a (kJ mol^{-1})	R^2	E_a (kJ mol^{-1})	R^2
ELO/DA$_{100}$ (control 1)	109	0.9175	115	0.9261
ELO/DA$_{50}$BA$_{50}$	**75**	**0.9996**	**82**	**0.9997**
ELO/BA$_{100}$ (control 2)	78	0.9992	85	0.9993

[a]R^2 is linear coefficient of fitting.

al.[29] synthesized epoxy resins by curing the diglycidyl ether of bisphenol A (DGEBA) with two different hardeners: SA and 4,4′-dithiodibutyric acid (DTDA). For these systems, the authors obtained E_a values of 99 kJ mol^{-1} for the DGEBA/SA system and 75 kJ mol^{-1} for the DGEBA/DTDA. A similar range of E_a values was reported by Mashouf Roudsari et al.,[49] who studied the curing kinetics of epoxy resins, prepared from SA and the blending of epoxy monomers containing DGEBA and ESO. A value of E_a of ∼64 kJ mol^{-1} is reported. In our case, a slightly higher value of E_a was obtained. The result is probably related to the lower reactivity and the steric hindrance of oxirane groups in ELO monomers, compared to those of diglycidyl ethers of DGEBA.

The combination of DA/BA (50/50) in the ELO curing mixture reduces the reaction activation energies with a significant decrease of 34 kJ mol^{-1} compared with the control 1 system (ELO/DA$_{100}$) and a slight decrease of 3 kJ mol^{-1} compared with the control 2 system (ELO/BA$_{100}$). This result highlights that by combining the two diacids, a higher reactivity is reached. The control 1 system has the highest activation energy of the curing because of the electron-donor character of the aliphatic chain. In fact, a previous study of our group[42] showed that the key step on the selectivity control of epoxy−acid propagation is the carboxylic−carboxylate complex equilibrium (Scheme 2). In the case of aliphatic acid (DA), the presence of electron-donating groups increases the electron density in the carboxylate anion (RCOO^{-}) and so destabilizes the carboxylate complex, restraining the formation of "reactive" species at the initial stage. This explanation confirms why the ELO/DA$_{100}$ system has a smaller enthalpy of cross-linking together with the occurrence of more pregnant secondary reactions in the systems containing the DA.

All of these findings are proof that the addition of an optimal amount of BA in the DA/ELO matrix could have a positive effect on the cross-linking reactivity. It provides an efficient way to increase the copolymerization reactivity, reducing curing temperature, time, and activation energy.

FT-IR Investigations. The FT-IR spectra of two carboxylic diacids (DA and BA) are shown in Figure S2, and the corresponding characteristic peak assignments are summarized in Table S5. Some common characteristic peaks are observed as the following absorption: O−H stretching in the region of 3300−2300 cm^{-1}; −C═O stretching at about 1678 cm^{-1}; C−O stretching in the 1320−1000 cm^{-1} region ;and the O−H bending at ∼1450 and ∼895 cm^{-1}.[8,50,51] In the case of aromatic acid, some signals attributed to the aromatic region exhibit at about ∼1586 and ∼750 cm^{-1} for ortho-substituted benzenes.

To evaluate the cross-linking reaction of ELO with the DA/BA mixture, we performed first the in situ FT-IR analysis during the curing reactions for all formulations. In Figure 3, the evolution of FT-IR spectra of the ELO/DA$_{30}$BA$_{70}$ mixture during curing is given as an example. These spectra reveal the gradual diminution of the −COOH absorptions at 1678 and 895 cm^{-1} together with that of oxirane C−O twin bands at 823 and 847 cm^{-1}. At the same time, the progressive increase of the peak at 3560 cm^{-1} is characteristic of the hydroxyls (−OH) and the appearance of the new ester's peak located at about 1710 cm^{-1} are observed. Moreover, the peak areas of the absorbance bands in the region from 1101 to 1242 cm^{-1} correspond to (C−O−C) ether linkage in the cross-linked epoxy network, which enhances significantly with increasing the temperature. This result indicates the cross-linking reaction of DCA in the ELO matrix, which is consistent with the aforementioned results obtained by DSC analyses.

A proposed mechanism of the EVO/DCA reaction in the presence of imidazole as the initiator is presented in Scheme 2a. In this mechanism, the IM initiates the reaction by a nucleophilic attack on the epoxy rings which are activated by the acid-H donor. This process leads to the formation of imidazolium−carboxylate complexes via hydrogen bonding in the transition state (Scheme 2a), propagating selectively the copolymerization.

Starting from the DSC data, the variations of fractional conversion as a function of temperature are obtained and are presented in Figure 4A. These representations show that the conversions increase slowly at the beginning of the curing reaction. However, after being heated to a given temperature, the reactivity increases very fast, then slows down before it levelled off at a certain value at the end. As already noted by the DSC results concerning the evolution of the T_{peak} on the five studied formulations, a similar tendency is obtained, meaning that to acquire the same fractional conversion, the needed reaction temperature to achieve the cross-linking increases in the order: ELO/DA$_{70}$BA$_{30}$ < ELO/DA$_{50}$BA$_{50}$ ≤
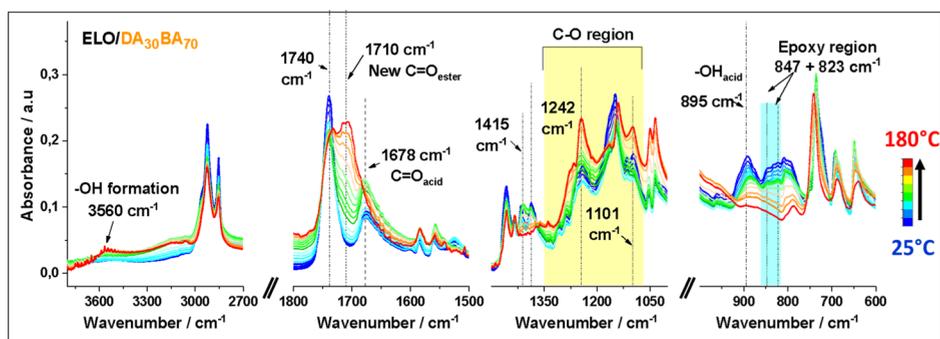
Figure 3. Evolution of FT-IR spectra of the ELO/DA$_{30}$BA$_{70}$ mixture during heating from 25 to 180 °C at 10 °C min^{-1}.
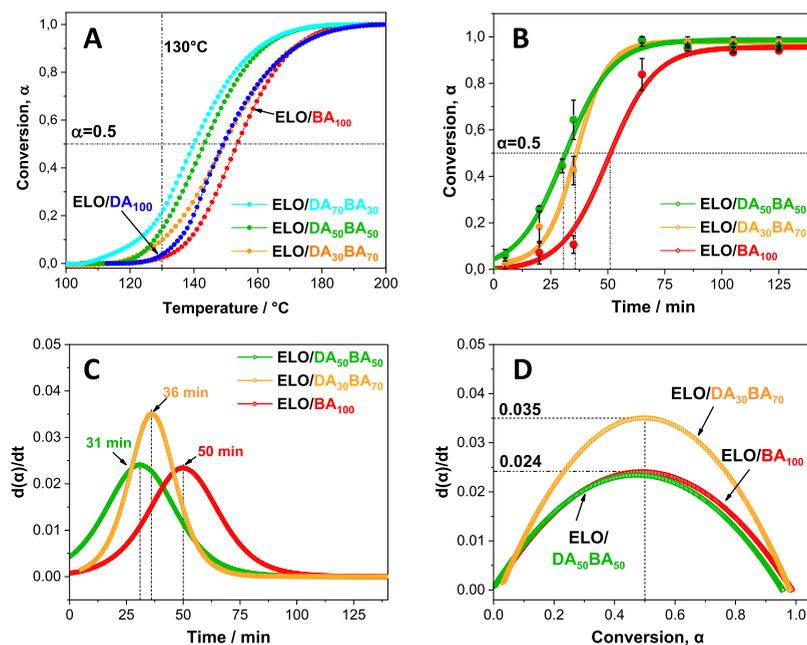
Figure 4. (A) Fractional conversion of the curing determined by dynamic DSC at 10 °C min⁻¹ heating rate; (B−D) kinetic study during the isothermal reaction ELO with the DA/BA mixture at 130 °C determined by FT-IR analysis: (B) conversion of epoxy groups (α) in function of time; (C) plot of $d(\alpha)/dt$ in function of time; and (D) plot of $d(\alpha)/dt$ in function of conversion (α).
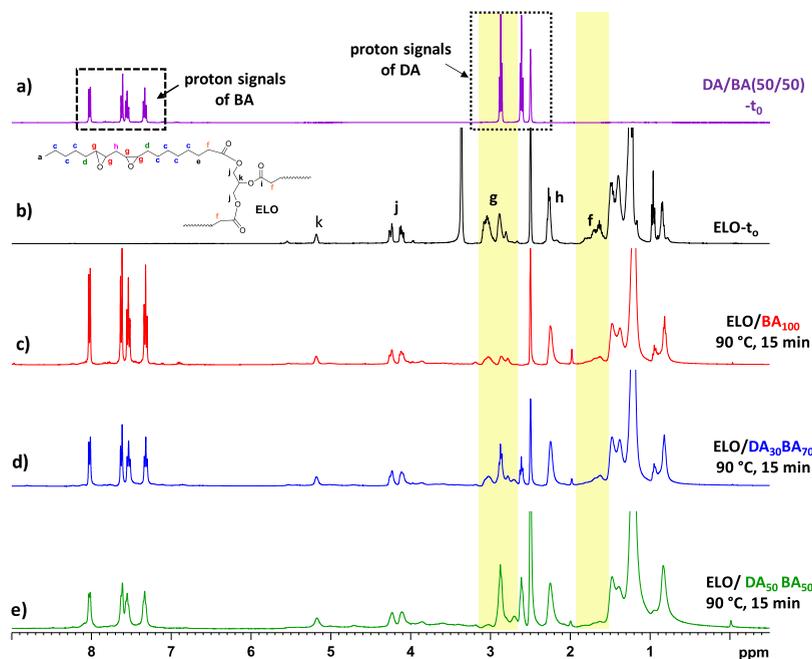
Figure 5. (a) ¹H NMR spectrum of the DA/BA (50/50) mixture at t_0, (b) ¹H NMR spectrum of ELO at t_0, and those of the 3 formulations previously heated at 90 °C for 15 min: (c) ELO/BA₁₀₀, (d) ELO/DA₃₀BA₇₀, and (e) ELO/DA₅₀BA₅₀. The protons from typical chemical structure of epoxidized oil are indicated in (b).

ELO/DA₃₀ BA₇₀ ≤ ELO/DA₁₀₀ < ELO/BA₁₀₀. Therefore, considering the kinetic of reaction dependence with the temperature, the order of reactivity is: ELO/DA₇₀BA₃₀ > ELO/DA₅₀BA₅₀ > ELO/DA₃₀ BA₇₀ > ELO/DA₁₀₀ > ELO/BA₁₀₀.

In fact, the DSC analyses allow obtaining kinetic parameters, which make it possible to simulate the curing. However, this technique gives information only about the overall process but not about the reaction mechanism and elemental reactions that occur during curing. In order to follow the structural changes in the functional groups of ELO/(DA/BA) formulations and

to respect the same experimental curing conditions, isothermal FT-IR analyses were monitored taking as an example ELO/DA₃₀BA₇₀/IM and collecting the spectra at different curing times at 130 °C (Figure S3). Figure S4 displays the isothermal FT-IR of the three formulations after 65 min of heating at 130 °C. This temperature was previously determined by DSC analysis.

The extent of cross-linking reaction was quantified by the peak area of epoxy group absorption at about 823 cm⁻¹ in reference to the peak at 1586 cm⁻¹, which corresponds to the
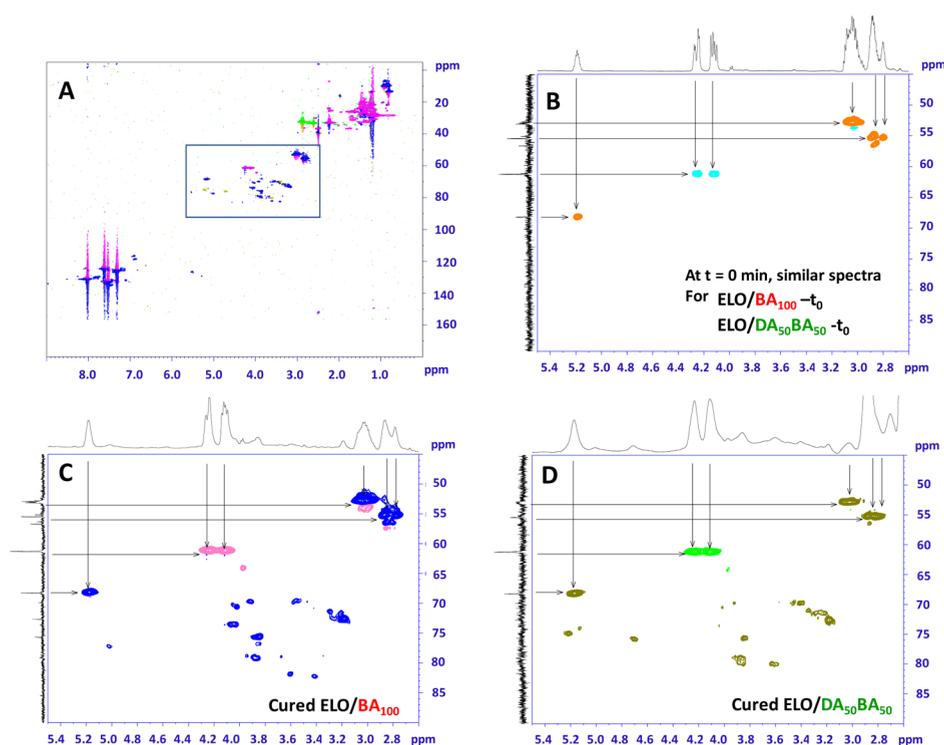
Figure 6. Multidimensional NMR investigations (A): superposition multiplicity-edited $^1H-^{13}C$ HSQC spectra of the ELO/BA$_{100}$ and ELO/DA$_{50}$BA$_{50}$ mixture cured at 90 °C for 15 min: positive peaks in blue, negative in purple for the ELO/BA$_{100}$ mixture, and positive peaks in sage green, negative in fluorescent green for ELO/DA$_{50}$BA$_{50}$.Enlargements in the $-$CH(OH) regions: (B) superposition spectra at the initial time for both formulations (positive peaks in orange, negative peaks in sky blue); (C): ELO/BA$_{100}$ (positive peaks in blue, negative in purple); and (D): ELO/DA$_{50}$BA$_{50}$ cured at 90 °C for 15 min (positive peaks in sage green, negative in fluorescent green).

C=C stretching of the BA aromatic ring. In fact, the conversion cannot be quantified in the case of ELO/DA$_{100}$ due to the absence of a reference peak. This is the same situation in the case the ELO/DA$_{70}$BA$_{30}$ system, where the reference has a very low intensity. The epoxy conversion (α) was calculated, using eq S3, as described in the Supporting Information. The corresponding results are given in Figure 4B. The relationships between the reaction rate (d(α)/dt) in function of time or conversion (α) are depicted in Figure 4C,D. From these data, we can observe that all the formulations achieve a full conversion ($\alpha \geq 0.97$). It can be noted from Figure 4D that the DA/BA (50/50) system shows kinetic similarities with the ELO/BA$_{100}$ system (control 2), both having the same dependence of reaction rate (d(α)/dt) in function of conversion (α). In contrast, in the case of the ELO/DA$_{30}$BA$_{70}$ system, the reaction rate is 1.5 times higher than those of ELO/DA$_{50}$BA$_{50}$ and ELO/BA$_{100}$ systems. This result is probably related to a higher reactivity of the diacid mixture versus oxirane groups and also to a better miscibility and compatibility between the reactants. As previously shown, the aromatic diacid has a higher reactivity toward the oxiran rings, but the aliphatic diacid is more compatible with the aliphatic chains of ELO.

At the initial time, the conversion of epoxy groups rises slowly with increasing reactivity in order: ELO/BA$_{100}$ < ELO/DA$_{30}$BA$_{70}$ < ELO/DA$_{50}$BA$_{50}$. After this first step of initiation consisting of the formation of "reactive" species, the propagation proceeds faster, the reaction rate increasing significantly to a maximum value, which is more rapid for the ELO/DA$_{50}$BA$_{50}$ system. A conversion $\alpha = 0.50$ is achieved after 50 min for ELO/BA$_{100}$ but after only 36 or 31 min,

respectively, for ELO/DA$_{30}$BA$_{70}$ and ELO/DA$_{50}$BA$_{50}$ systems. These results highlight that the BA + DA mixtures are more reactive than the system with BA alone, being characterized by reduced curing temperature and time. This outcome corroborates with the aforementioned results obtained by nonisothermal DSC analyses and NMR experiments (Figure S15).

NMR Investigations. To highlight the structural modifications occurring during copolymerization, NMR investigations were performed. For this, we compared the ^1H NMR spectra of initial reactants DA/BA (50/50) and ELO at the initial time with those of the three formulations, previously heated in an oven at 90 °C for 15 min and thereafter dissolved in DMSO-d_6 (Figure 5). As seen in Figure 5, some new $-$CH(OH) proton signals in the region 3.5−5.0 ppm are observed. At the same time, the proton at 2.7−3.30 ppm and between 1.88 and 1.55 ppm assigned to the oxirane ring (H$_g$) and those of−CH$_2$ in the α-position of epoxides decreased significantly. The total disappearance of these two peaks is noticed when the curing time increases. These results are proof indicating the ring opening of epoxy functions (ELO), and therefore the formation of β-hydroxyl esters.

To confirm the previous attribution and to follow the reactivity study, a multidimensional NMR investigation was performed in ELO/BA$_{100}$ at t_0 (Figure S5) and that of the mixture cured at 90 °C for 15 min (Figure S6). The results were compared with the ELO/DA$_{50}$BA$_{50}$ mixture cured at 90 °C for 15 min (Figure S7) and at 170 °C for 10 min (Figure S8). The multiplicity-edited $^1H-^{13}C$ HSQC spectrum shows the correlations between protons and carbons generating

G

Scheme 3. Exchange Reactions between BA and DA
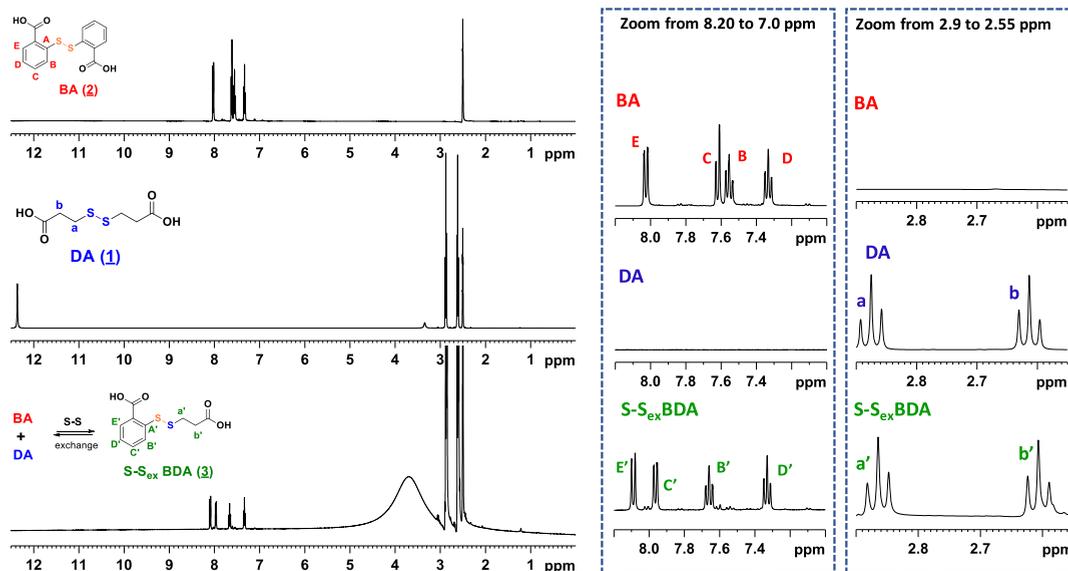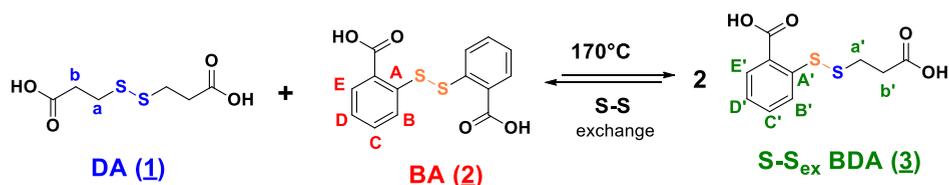
Figure 7. ^{1}H NMR spectrum of the mixture of two diacids (DA + BA), heated at 170 °C for 10 min, in comparison with that of initial BA and DA.
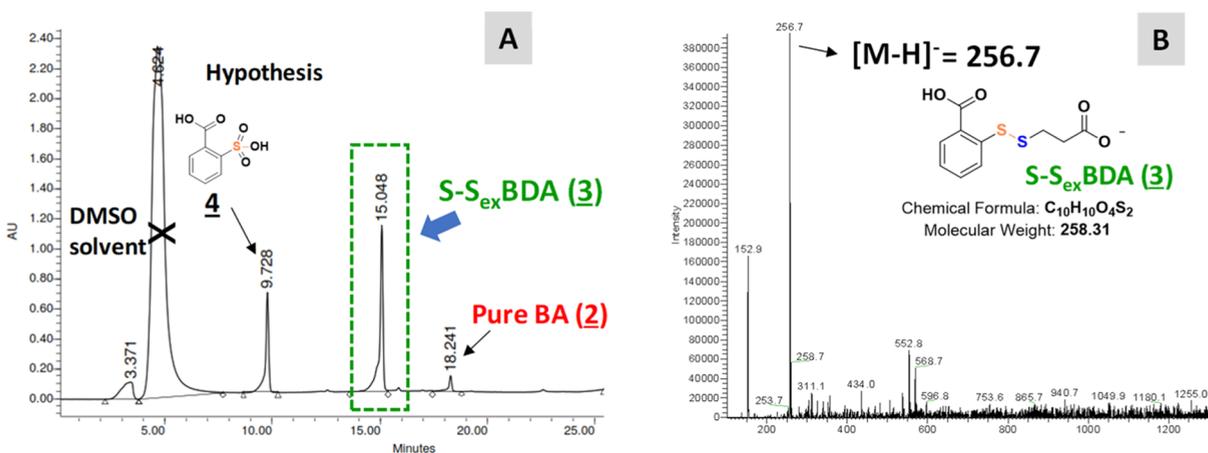
Figure 8. (A) HPLC chromatogram and (B) ESI-MS spectrum of the mixture of two diacids (DA + BA), heated at 170 °C for 10 min confirming the presence of the product S−S$_{ex}$ BDA (**3**) generated by the disulfide exchange between the two structures.

opposite signs between peaks of CH_2 (negative) and CH/CH_3 (positive).

Figure 6 exhibits the HSQC spectra of the samples before becoming insoluble in the DMSO-d_6 solvent in comparison with that at t_0. The first notable difference, as previously noticed by ^{1}H NMR, is the decrease, but still present with small intensity, of the −H$_g$ resonance at 2.8−3.1 ppm from the oxirane signal, confirmed by the cross-peak at $^{13C}\delta$ = 54−58 ppm (C_g). This result suggests the occurrence of epoxide ring opening together with the presence of some unreacted oxiranes still present after heating at 90 °C for 15 min. At the same time, new cross-peaks appear at around $^{1H}\delta$ = 3.3−4.6 ppm and $^{13C}\delta$ = 70.0−85.0 ppm (Figure 6C,D), resulting from the

possible reactions, as exposed in Scheme 2. The structural evolution is also accompanied by a shift of methylene functions in the α-position of epoxies rings from 1.8−1.5 to 1.5−1.3 ppm in ^{1}H NMR and from 11.2−14.8 to 25.0−33.0 ppm in ^{13}C NMR. As previously reported,[52] the ELO homopolymerization can be identified by the presence of the cross-peaks (positive) at the chemical shift around $^{1H}\delta$ = 2.8 ppm and $^{13C}\delta$ = 55 ppm. Regarding the HSQC NMR spectra of the reacted ELO/BA$_{100}$ (Figure 6C) and ELO/DA$_{50}$ BA$_{50}$ (Figure 6D) systems, we do not observe these cross-peaks at the conditions we used for conducting the reactions, that is, heating at 90 °C for 15 min. The result indicates and confirms the previous FT-IR results showing that in both systems: ELO/BA$_{100}$ and ELO/DA$_{50}$BA$_{50}$

occurred dominantly the epoxy–acid copolymerization and no epoxide homopolymerization, when reacted at 90 °C for 15 min. Moreover, in the case of the 50/50 (BA/DA) mixture, new cross-peaks appear in comparison to ELO/BA$_{100}$ (Figure 6C,D). This result suggests that the cross-linking of ELO with DA or BA occurs simultaneously.

Aromatic Versus Aliphatic Disulfide Exchange. To demonstrate that the addition of BA in DA/ELO curing formulation can accelerate the disulfide metathesis reaction, enhancing the reprocessing ability *via* the introduction of aromatic disulfide bonds with a lower BDE, a mixture of both diacids DA and BA with the ratio in mole (r = BA/DA = 1/ 10), in excess of DA because of its lower melting temperature, was heated in an oven at 170 °C for 10 min, and then the obtained product was analyzed using NMR spectroscopy, HPLC, and LC−MS methods. The disulfide metathesis reaction between BA and DA is depicted in Scheme 3. The obtained results are given in Figures 7 and 8.

The formation of a new product, assigned to the S−S exchange reaction, is proven through the change of signals in the ^{1}H and ^{13}C NMR spectra, especially for the proton of the benzene moiety from 8.2 to 7.0 ppm, as shown in Figure 7. The ^{1}H NMR signals assigned as B, C, D, and E were attributed to the proton signals of BA (**2**), the a, b were ascribed to DA (**1**), while B′, C′, D′, E′, a′, b′ were attributed to the signals of formed exchanged product S−S$_{ex}$BDA (**3**). This attribution is in good agreement with Yang *et al.*,[53] who identified the chemical structure of compound (**3**), prepared from the one-pot synthesis of unsymmetrical disulphides using trichloroisocyanuric acid with the help of NMR. It can be noted also that, after 10 min at 170 °C, the majority of BA (limiting reactant) was converted, confirmed by the quasi-total disappearance of BA proton signals.

In order to confirm the assumption that the aromatic− aliphatic disulfide exchange was carried out and to validate the formation of the S−S$_{ex}$BDA compound, HPLC and LC−MS experiments were performed. The corresponding chromato- graph and spectrum are depicted in Figure 8. As expected, the ESI-MS (Figure 8B) spectrum confirms the presence of S− S$_{ex}$BDA, at which the exact mass calculated for [M − H]$^-$, 256.9948; found for, 256.7.

In fact, BA was analyzed in the same manner by HPLC. Its retention time (t_R) was detected at 18.2 min. Considering the obtained HPLC chromatograph of the mixture (Figure 8A) and based on the polarity theory, we can attribute that the retention time was about 15.05 min for the S−S$_{ex}$ BDA product, while the peak at 9.73 min can be assigned to the formation of the secondary product [2-sulfobenzoic acid (**4**)] probably due to the oxidation of phenyl sulfide radicals in air. It should be noted that after 10 min, 6.5% of BA are still present in the mixture, as presented in Figure 8A, at a retention time of 18.2 min. This observation is confirmed also by the presence of characteristic signals of BA in the ^{1}H NMR spectrum. We can highlight that after heating the mixture of two acids at 170 °C for 10 min, a reaction exchange occurred reaching a 60% conversion, the value was calculated by area peaks.

Now, the question arises on the influence of these dynamic S−S bonding on the reactivity of two hardeners versus ELO monomer *via* the epoxy–acid reaction, and if the exchange reaction will occur also during the curing at 130 °C. To answer this question, an equimolar mixture of DA/BA (50/50) was dissolved in DMSO-d_6, then heated at 130 °C (*i.e.*, the curing

temperature) for 2 and 5 h. The collecting samples were analyzed by ^{1}H and ^{13}C NMR. The corresponding results are displayed in Figure 9. The literature reports[54] that the presence
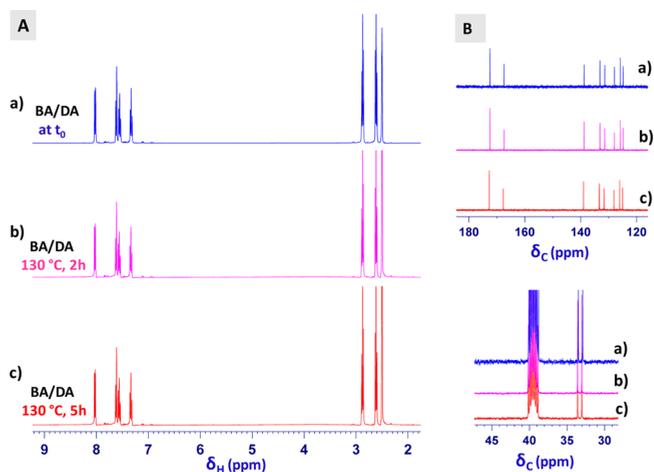
Figure 9. (A) ^{1}H NMR spectrum and (B) ^{13}C NMR of the mixture of two diacids (BA/DA: 50/50), heated at curing temperature at 130 °C for 2 and 5 h in comparison with that of initial BA and DA. No difference detected.

of dynamic S−S bonding in the β position of the carboxylic group can increase the reactivity of acid proton toward the epoxy group, and therefore, produces an increase of reactivity. The ^{1}H and ^{13}C spectra of the mixture BA/DA are shown in Figure 9A,B respectively. At initial time (t_0), the signals correspond only to the contribution from BA ($^{1H}\delta$ = 8.22−7.27 ppm) and DA ($^{1H}\delta$ = 2.92−2.55 ppm). The chemical shifts and the corresponding peak assignments of starting materials (BA, DA) are listed in the Supporting Information (Figures S9−S13).

Interestingly, it can be seen from Figure 9 that all spectra are superposed, no new signals were detected in the BA/DA mixture, even if this was heated for 5 h at 130 °C. It indicates no interaction, in particular, no exchange reaction between BA and DA occurs, therefore dismissing the formation of other reactions during the cross-linking process. This attribution is confirmed by Imbernon *et al.*,[55] who studied a dynamic covalent network by cross-linking the epoxidized natural rubber (ENR) with a disulfide containing carboxylic diacid in comparison with the corresponding single aliphatic diacid (without the presence of S−S bonding). The authors showed that the obtained polymer networks were able to rearrange only at higher temperatures, above 150 °C. For their system, it was needed to cure ENR with DCA at high temperatures (180 °C). The authors reported that during the cross-linking reaction, disulfide bonds could break either into radicals or into thiols. These intermediates could not only react with another disulfide bond (reversible covalent chemistry) but could also react with the other functional groups of epoxy monomers and/or could easily oxidized.

Glass Transition Determined by DSC. One of the most challenging aspects in thermosetting resin synthesis is the monomer/hardener miscibility and phase separation during curing. In order to evaluate this aspect, the glass transition (T_g) of the prepared materials was analyzed by DSC measurement with heat-cooling (at 10 °C min^{-1}) in the range from −60 to 180 °C. Interestingly, only a single peak was detected for all of

five formulations. It can be the sign of a good physico-chemical compatibility between the curing system components. By adding in the ELO, a hardener with a melting temperature of 155 °C (DA), lower than that of BA (287 °C), and the presence of IM as the initiator give a combination that can help to better dissolve and disperse BA in the curing mixture.

Concerning the thermoset properties, the Figures 10 and S14 show that the addition of BA in the DA mixture increases
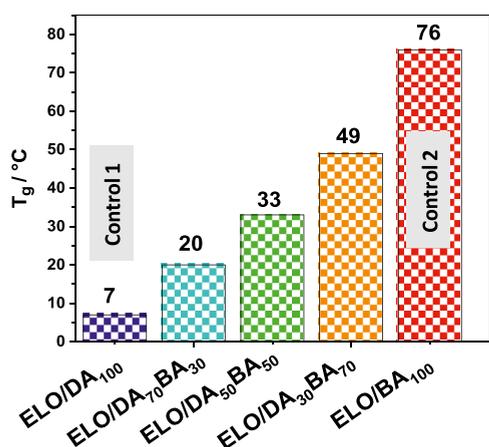
Figure 10. Glass transitions of cross-linked materials obtained *via* the DSC experiment.

progressively the T_g of the cured materials from 7 °C (ELO/DA$_{100}$, control 1) to 76 °C (ELO/BA$_{100}$, control 2). A similar range of T_g was reported by Ding *et al.*,[8] who studied the curing of ELO with aliphatic DCA. According to the authors, the T_g varied from −15.7 to 7 °C, depending on the aliphatic chain length of the hardener. Comparing the results reported by Gobin *et al.*[56] on the curing of epoxidized broccoli oil with *o*-phenylene diacetic acid, obtaining a thermoset with a T_g of 16 °C, our materials exhibit much higher T_g values. This indicates that the addition of BA in the DA/ELO matrix produces a significant increase of the T_g value, therefore, of mechanical properties. As expected, the highest T_g value (76 °C) was obtained for the ELO/BA$_{100}$ system.

CONCLUSIONS

In this work, novel dual dynamic epoxy resins were developed, and moreover, we have demonstrated for the first time that by combining aliphatic and aromatic diacids the reactivity increases, particularly for ELO/DA$_{50}$BA$_{50}$ formulation. In terms of sustainable development, this combination of aromatic/aliphatic diacids significantly decreases the reaction temperature, activation energy, and therefore the energy costs. At the same time, it helps to promote and generate a homogenous network polymer. Moreover, the combination of hard and soft segments in the network would favor superior thermomechanical performances of these thermosets, a study that will be deeply investigated in a future work.

The addition of BA as an aromatic diacid in the DA/ELO matrix not only increases the glass transition of the network but can accelerate the disulfide metathesis reaction, therefore enhancing the reprocessing ability. The exchange reaction between the 2 hardeners containing dynamic S−S bonds was proved to occur at 170 °C (the reprocessing temperature) by a combination of NMR, HPLC, and LC−MS analyses. The obtained results show clearly that no exchange reaction

between BA and DA occurs during the heating at the curing temperature (130 °C) of both diacids, therefore dismissing the occurrence of exchange reactions during cross-linking. Taking advantage of these results, we can anticipate that incorporating disulfide moieties from both BA and DA to an epoxy resin will benefit various industries that require robust materials capable of on-demand degradation, recycling applications, and self-healing capabilities.

ASSOCIATED CONTENT

Ⓢ Supporting Information

The Supporting Information is available free of charge at https://pubs.acs.org/doi/10.1021/acsabm.0c00788.

Chemical reagents, sample preparation, and analytical methods. FT-IR, ^{1}H NMR, and ^{13}C NMR spectra of starting materials, evolution of FT-IR spectra at different curing times and temperatures, 2D multiplicity-edited ^{1}H−^{13}C HSQC spectra of the ELO/BA$_{100}$ and ELO/BA$_{50}$DA$_{50}$ at a initial time at 90 °C for 15 min, and glass transitions of thermosets by DSC (PDF)

AUTHOR INFORMATION

Corresponding Author

Alice Mija − *Université Côte d'Azur, Institut de Chimie de Nice, UMR 7272—CNRS, 06108 Nice Cedex 2, France;* ⓘ orcid.org/0000-0001-5208-5956; Email: Alice.MIJA@univ-cotedazur.fr

Authors

Thi-Nguyet Tran − *Université Côte d'Azur, Institut de Chimie de Nice, UMR 7272—CNRS, 06108 Nice Cedex 2, France*

Chiara Di Mauro − *Université Côte d'Azur, Institut de Chimie de Nice, UMR 7272—CNRS, 06108 Nice Cedex 2, France*

Samuel Malburet − *Specific Polymers, 34160 Castries, France;* ⓘ orcid.org/0000-0002-4224-9520

Alain Graillot − *Specific Polymers, 34160 Castries, France*

Complete contact information is available at:
https://pubs.acs.org/10.1021/acsabm.0c00788

Notes

The authors declare no competing financial interest.

ACKNOWLEDGMENTS

ABBREVIATIONS

EVO, epoxidized vegetable oil; ELO, epoxidized linseed oil; DCA, dicarboxylic acids; ArDCA, aromatic dicarboxylic acids; BA, 2,2′-dithiodibenzoic acid; DA, 3,3′-dithiodipropionic acid; IM, imidazole; FT-IR, Fourier transform infrared spectroscopy; DSC, differential scanning calorimetry; HPLC, high performance liquid chromatography; LC−MS, liquid chromatography−mass spectrometry; HSQC, multiplicity-edited ^{1}H−^{13}C heteronuclear single quantum coherence; *vs*, versus

REFERENCES

(1) Pin, J.-M.; Guigo, N.; Vincent, L.; Sbirrazzuoli, N.; Mija, A. Inside Cover: Copolymerization as a Strategy to Combine Epoxidized

Linseed Oil and Furfuryl Alcohol: The Design of a Fully Bio-Based Thermoset. *ChemSusChem* **2015**, *8*, 4098.

(2) Ramon, E.; Sguazzo, C.; Moreira, P. A Review of Recent Research on Bio-Based Epoxy Systems for Engineering Applications and Potentialities in the Aviation Sector. *Aerospace* **2018**, *5*, 110.

(3) Mora, A.-S.; Tayouo, R.; Boutevin, B.; David, G.; Caillol, S. Vanillin-derived amines for bio-based thermosets. *Green Chem.* **2018**, *20*, 4075−4084.

(4) Dhers, S.; Vantomme, G.; Avérous, L. A fully bio-based polyimine vitrimer derived from fructose. *Green Chem.* **2019**, *21*, 1596−1601.

(5) Shibata, M.; Ohkita, T. Fully biobased epoxy resin systems composed of a vanillin-derived epoxy resin and renewable phenolic hardeners. *Eur. Polym. J.* **2017**, *92*, 165−173.

(6) La Rosa, A.; Blanco, I.; Banatao, D.; Pastine, S.; Björklund, A.; Cicala, G. Innovative chemical process for recycling thermosets cured with recyclamines by converting Bio-Epoxy Composites in Reusable Thermoplastic-An LCA Study. *Materials* **2018**, *11*, 353.

(7) Stemmelen, M.; Lapinte, V.; Habas, J.-P.; Robin, J.-J. Plant oil-based epoxy resins from fatty diamines and epoxidized vegetable oil. *Eur. Polym. J.* **2015**, *68*, 536−545.

(8) Ding, C.; Shuttleworth, P. S.; Makin, S.; Clark, J. H.; Matharu, A. S. New insights into the curing of epoxidized linseed oil with dicarboxylic acids. *Green Chem.* **2015**, *17*, 4000−4008.

(9) Tan, S. G.; Chow, W. S. Curing Characteristics and Thermal Properties of Epoxidized Soybean Oil Based Thermosetting Resin. *J. Am. Oil Chem. Soc.* **2011**, *88*, 915−923.

(10) Altuna, F. I.; Pettarin, V.; Williams, R. J. J. Self-healable polymer networks based on the cross-linking of epoxidised soybean oil by an aqueous citric acid solution. *Green Chem.* **2013**, *15*, 3360−3366.

(11) Park, S.-J.; Jin, F.-L.; Lee, J.-R. Thermal and mechanical properties of tetrafunctional epoxy resin toughened with epoxidized soybean oil. *Mater. Sci. Eng., A* **2004**, *374*, 109−114.

(12) Altuna, F. I.; Espósito, L. H.; Ruseckaite, R. A.; Stefani, P. M. Thermal and mechanical properties of anhydride-cured epoxy resins with different contents of biobased epoxidized soybean oil. *J. Appl. Polym. Sci.* **2011**, *120*, 789−798.

(13) Zeng, R.-T.; Wu, Y.; Li, Y.-D.; Wang, M.; Zeng, J.-B. Curing behavior of epoxidized soybean oil with biobased dicarboxylic acids. *Polym. Test.* **2017**, *57*, 281−287.

(14) Pietroluongo, M.; Padovano, E.; Frache, A.; Badini, C. Mechanical recycling of an end-of-life automotive composite component. *Sustainable Mater. Technol.* **2020**, *23*, No. e00143.

(15) Rybicka, J.; Tiwari, A.; Alvarez Del Campo, P.; Howarth, J. Capturing composites manufacturing waste flows through process mapping. *J. Clean. Prod.* **2015**, *91*, 251−261.

(16) Perrin, D.; Clerc, L.; Leroy, E.; Lopez-Cuesta, J.-M.; Bergeret, A. Optimizing a recycling process of SMC composite waste. *Waste Manag.* **2008**, *28*, 541−548.

(17) Badia, J. D.; Gil-Castell, O.; Ribes-Greus, A. Long-term properties and end-of-life of polymers from renewable resources. *Polym. Degrad. Stab.* **2017**, *137*, 35−57.

(18) Hong, M.; Chen, E. Y.-X. Chemically recyclable polymers: a circular economy approach to sustainability. *Green Chem.* **2017**, *19*, 3692−3706.

(19) Ravi, V. Evaluating overall quality of recycling of e-waste from end-of-life computers. *J. Clean. Prod.* **2012**, *20*, 145−151.

(20) Otheguy, M. E.; Gibson, A. G.; Findon, E.; Cripps, R. M.; Mendoza, A. O.; Castro, M. T. A. Recycling of end-of-life thermoplastic composite boats. *Plast., Rubber Compos.* **2009**, *38*, 406−411.

(21) Roy, N.; Bruchmann, B.; Lehn, J.-M. DYNAMERS: dynamic polymers as self-healing materials. *Chem. Soc. Rev.* **2015**, *44*, 3786−3807.

(22) Burattini, S.; Greenland, B. W.; Merino, D. H.; Weng, W.; Seppala, J.; Colquhoun, H. M.; Hayes, W.; Mackay, M. E.; Hamley, I. W.; Rowan, S. J. A Healable Supramolecular Polymer Blend Based on Aromatic $\pi−\pi$ Stacking and Hydrogen-Bonding Interactions. *J. Am. Oil Chem. Soc.* **2010**, *132*, 12051−12058.

(23) Ohishi, T.; Iki, Y.; Imato, K.; Higaki, Y.; Takahara, A.; Otsuka, H. Insertion Metathesis Depolymerization of Aromatic Disulfide-containing Dynamic Covalent Polymers under Weak Intensity Photoirradiation. *Chem. Lett.* **2013**, *42*, 1346−1348.

(24) Amamoto, Y.; Kamada, J.; Otsuka, H.; Takahara, A.; Matyjaszewski, K. Repeatable Photoinduced Self-Healing of Covalently Cross-Linked Polymers through Reshuffling of Trithiocarbonate Units. *Angew. Chem., Int. Ed.* **2011**, *50*, 1660−1663.

(25) Matxain, J. M.; Asua, J. M.; Ruipérez, F. Design of new disulfide-based organic compounds for the improvement of self-healing materials. *Phys. Chem. Chem. Phys.* **2016**, *18*, 1758−1770.

(26) Kloxin, C. J.; Bowman, C. N. Covalent adaptable networks: smart, reconfigurable and responsive network systems. *Chem. Soc. Rev.* **2013**, *42*, 7161−7173.

(27) Lei, Z. Q.; Xiang, H. P.; Yuan, Y. J.; Rong, M. Z.; Zhang, M. Q. Room-Temperature Self-Healable and Remoldable Cross-linked Polymer Based on the Dynamic Exchange of Disulfide Bonds. *Chem. Mater.* **2014**, *26*, 2038−2046.

(28) Ruiz de Luzuriaga, A.; Martin, R.; Markaide, N.; Rekondo, A.; Cabañero, G.; Rodríguez, J.; Odriozola, I. Epoxy resin with exchangeable disulfide crosslinks to obtain reprocessable, repairable and recyclable fiber-reinforced thermoset composites. *Mater. Horiz.* **2016**, *3*, 241−247.

(29) Chen, M.; Zhou, L.; Wu, Y.; Zhao, X.; Zhang, Y. Rapid Stress Relaxation and Moderate Temperature of Malleability Enabled by the Synergy of Disulfide Metathesis and Carboxylate Transesterification in Epoxy Vitrimers. *ACS Macro Lett.* **2019**, *8*, 255−260.

(30) Canadell, J.; Goossens, H.; Klumperman, B. Self-Healing Materials Based on Disulfide Links. *Macromolecules* **2011**, *44*, 2536−2541.

(31) Gong, J. P. Why are double network hydrogels so tough? *Soft Matter* **2010**, *6*, 2583−2590.

(32) Imbernon, L.; Pire, M.; Oikonomou, E. K.; Norvez, S. Semi-interpenetrating Networks in Blends of Epoxidized Natural Rubbers. *Macromol. Chem. Phys.* **2013**, *214*, 806−811.

(33) Black, S. P.; Sanders, J. K. M.; Stefankiewicz, A. R. Disulfide exchange: exposing supramolecular reactivity through dynamic covalent chemistry. *Chem. Soc. Rev.* **2014**, *43*, 1861−1872.

(34) Azcune, I.; Odriozola, I. Aromatic disulfide crosslinks in polymer systems: Self-healing, reprocessability, recyclability and more. *Eur. Polym. J.* **2016**, *84*, 147−160.

(35) Di Mauro, C.; Malburet, S.; Genua, A.; Graillot, A.; Mija, A. Sustainable series of new epoxidized vegetable oils-based thermosets with chemical recycling properties. *Biomacromolecules* **2020**, *21*, 3923−3935.

(36) Mauro, C. D.; Genua, A.; Mija, A. Building thermally and chemically reversible covalent bonds in vegetable oils based epoxy thermosets. Influence of epoxy-hardener ratio to promote recyclability. *Mat. Adv.* **2020**, *1*, 1788−1798.

(37) Di Mauro, C.; Tran, T.-N.; Graillot, A.; Mija, A. Enhancing the Recyclability of a Vegetable Oil-Based Epoxy Thermoset through Initiator Influence. *ACS Sustain. Chem. Eng.* **2020**, *8*, 7690−7700.

(38) Ricciardi, F.; Romanchick, W. A.; Joullié, M. M. Mechanism of imidazole catalysis in the curing of epoxy resins. *J. Polym. Sci., Polym. Chem. Ed.* **1983**, *21*, 1475−1490.

(39) Heise, M. S.; Martin, G. C. Curing mechanism and thermal properties of epoxy-imidazole systems. *Macromolecules* **1989**, *22*, 99−104.

(40) Yang, S.; Zhang, Q.; Hu, Y.; Ding, G.; Wang, J. Synthesis of maleimide modified imidazole derivatives and their application in one-component epoxy resin systems. *Mater. Lett.* **2019**, *234*, 379−383.

(41) Liu, L.; Li, M. Curing mechanisms and kinetic analysis of DGEBA cured with a novel imidazole derivative curing agent using DSC techniques. *J. Appl. Polym. Sci.* **2010**, *117*, 3220−3227.

(42) Tran, T.-N.; Mauro, C. D.; Graillot, A.; Mija, A. Chemical Reactivity and the Influence of Initiators on the Epoxidized Vegetable Oil/Dicarboxylic Acid System. *Macromolecules* **2020**, *53*, 2526−2538.

(43) Boquillon, N.; Fringant, C. Polymer networks derived from curing of epoxidised linseed oil: influence of different catalysts and anhydride hardeners. *Polymer* **2000**, *41*, 8603−8613.

(44) Falco, G.; Sbirrazzuoli, N.; Mija, A. Biomass derived epoxy systems: From reactivity to final properties. *Mater. Today Commun.* **2019**, *21*, 100683.

(45) Kissinger, H. E. Reaction Kinetics in Differential Thermal Analysis. *Anal. Chem.* **1957**, *29*, 1702−1706.

(46) Ozawa, T. Kinetic analysis of derivative curves in thermal analysis. *J. Therm. Anal.* **1970**, *2*, 301−324.

(47) Haines, P. J. *Principles of Thermal Analysis and Calorimetry*, Book; RSC, 2002; pp 55−93.

(48) Mittal, V. *Thermoset Nanocomposites*; John Wiley & Sons: Book, 2013.

(49) Mashouf Roudsari, G.; Mohanty, A. K.; Misra, M. Study of the Curing Kinetics of Epoxy Resins with Biobased Hardener and Epoxidized Soybean Oil. *ACS Sustain. Chem. Eng.* **2014**, *2*, 2111−2116.

(50) Max, J.-J.; Chapados, C. Infrared Spectroscopy of Aqueous Carboxylic Acids: Comparison between Different Acids and Their Salts. *J. Phys. Chem. A* **2004**, *108*, 3324−3337.

(51) Tan, S. G.; Chow, W. S. Thermal properties of anhydride-cured bio-based epoxy blends. *J. Therm. Anal. Calorim.* **2010**, *101*, 1051−1058.

(52) Pin, J.-M.; Guigo, N.; Vincent, L.; Sbirrazzuoli, N.; Mija, A. Copolymerization as a Strategy to Combine Epoxidized Linseed Oil and Furfuryl Alcohol: The Design of a Fully Bio-Based Thermoset. *ChemSusChem* **2015**, *8*, 4149−4161.

(53) Yang, F.; Wang, W.; Li, K.; Zhao, W.; Dong, X. Efficient one-pot construction of unsymmetrical disulfide bonds with TCCA. *Tetrahedron Lett.* **2017**, *58*, 218−222.

(54) Jaillet, F.; Desroches, M.; Auvergne, R.; Boutevin, B.; Caillol, S. New biobased carboxylic acid hardeners for epoxy resins. *Eur. J. Lipid Sci. Technol.* **2013**, *115*, 698−708.

(55) Imbernon, L.; Oikonomou, E. K.; Norvez, S.; Leibler, L. Chemically crosslinked yet reprocessable epoxidized natural rubber via thermo-activated disulfide rearrangements. *Polym. Chem.* **2015**, *6*, 4271−4278.

(56) Gobin, M.; Loulergue, P.; Audic, J.-L.; Lemiègre, L. Synthesis and characterisation of bio-based polyester materials from vegetable oil and short to long chain dicarboxylic acids. *Ind. Crop. Prod.* **2015**, *70*, 213−220.